

Journal of Climate Change, Vol. 9, No. 4 (2023), pp. 1-11. DOI 10.3233/JCC230027

Palaeoenvironmental and Palaeoclimatic Conditions in the Bhimtal Valley, Kumaun Lesser Himalaya, Between 40 and 24 ka Using Granulometric Analysis

B.S. Kotlia¹*, Manmohan Kukreti¹, Harish Bisht¹, Biswajit Palar², Martin Seiler³, Marie-Josée Nadeauc³, A.K. Singh⁴, L.M. Joshi⁵, Anupam Sharma⁶, Rajkumar Kashyap⁷, Pooja Chand¹, Kalpana Gururani¹ and Abhishek Mehra¹

¹Centre of Advanced Study in Geology, Kumaun University, Nainital – 263001, India
²Centre for Ocean, River, Atmosphere and Land Sciences, Indian Institute of Technology, Kharagpur – 721302, India
³The National Laboratory for Age Determination, Norwegian University of Science and Technology, NTNU University Museum, Trondheim, Norway

Received September 24, 2023; revised and accepted October 16, 2023

Abstract: In this research, we conducted a detailed granulometric analysis of 9.5 m thick palaeolake succession, exposed at Bilaspur (Bhimtal) in the Kumaun Lesser Himalaya to reconstruct the palaeoenvironmental and palaeoclimatic conditions. We carried out statistical parameters of grain-size data (i.e., standard deviation, kurtosis, and skewness, bivariate plots), and end member modelling analysis (EMMA) and our study reveal sediment's unimodal and bimodal nature, deposited via fluvial action under low to high energy environmental conditions since the origin of the lake. Some parts of the deposit show poorly sorted and mixed character (leptokurtic to platykurtic) of sediments, indicating that the sediments were primarily transported from the proximal area of the lake basin under low-energy environmental conditions. The finely skewed and poorly sorted sediments show different modes of grain size distribution, which are attributed to fluctuations in the hydrodynamic conditions of the lake. The arid climatic conditions prevailed in the valley from ca. 42 to 40 ka BP, followed by warm and moist conditions from ca. 40 to 39 ka BP. The arid conditions under the low rainfall regime were experienced by the valley from ca. 39 to 30 ka BP, while it exercised another episode of moist and warmer conditions from ca. 30 to 24 ka BP. Further, the end-Member Modelling Analysis (EMMA) shows four end members (EM1-EM4) with different climatic conditions during the deposition, e.g., clay to fine silt-size particles reflecting higher lake levels under warm-wet climatic conditions, coarse silt fraction representing moderate energy conditions, and fine to coarse sand fractions indicating shallow lake-level conditions in the arid climatic conditions as well higher energy flow. The interpretation of energy conditions in the lake and catchment area by using various methods reveals different palaeoenvironmental conditions during the sediment deposition.

Keywords: Kumaun Lesser Himalaya; Palaeolake deposits; Granulometric analysis; Statistical parameters; End Member Modeling Analysis (EMMA).

Introduction

Lakes are a valuable source of continuous sedimentary archives as well as complex systems that can offer diverse physical, chemical, and biological data (Adrian et al., 2009) which can be utilised as a proxy to quantify the response of the ecosystem, earth's surface processes, and anthropogenic influences on the lake. As the internal feedback mechanism of lakes is governed by various factors such as catchment size, geology, climate, morphometry, land use and land cover in the surrounding area, it is essential to consider parameters like sedimentation rate, organic productivity, lake bottom sediment texture and bathymetry to understand the dynamics of the lake (Flemming, 2007). Among the different natural records, such as deep-sea sediments, loess, ice cores, coral, peat, varves and tree rings, etc., the lacustrine material stands out with a large geographic distribution, extensive long time span with excellent continuous records of layering of sedimentations and a wealth of environmental data. As a result, it plays a crucial function as a primary indicator for understanding global climate changes over a range of different time intervals (Chen et al., 2004). Sediment deposition in lakes is often continuous, offering valuable insights into significant climatic fluctuations in the past (Kotlia et al., 2023). The Himalayan lakes are sensitive indicators of climatic as well as environmental changes with implications at both regional and global levels. These serve as important archives for palaeoclimatic studies, storing valuable information about climatic history.

A granulometric analysis is an essential sedimentological tool to interpret the depositional environment and hydrodynamic conditions. The sizes of particles are intricately connected to factors such as turbulence, wave energy and proximity to the shoreline, sediment transport processes, energy levels and erosional strength, as coarsening or fining of the particles can signify intensified or weakening erosion strength (Wang et al., 2016). Generally, larger grain sizes are associated with higher energy conditions during sediment production or transport, while smaller grain sizes suggest lower energy levels. These changes in particle size reflect the dynamics of erosion processes occurring within the lake and its surrounding catchment area. During periods of higher lake levels, finer sediment particles tend to be deposited in the central part of the lake, while coarser particles are typically confined to the near shore zone (Rawat et al., 2021). Conversely, the lake's center would be relatively closer under lower lake-level conditions, and coarser particles would be deposited under high-energy conditions (Bird et al., 2014; Rawat et al., 2021). Thus, variations in grain size within the sediment over time, particularly an increase in the presence of sand, can indicate periods of drier and warmer climates, corresponding to lower lake levels. Conversely, a decrease in sand content may indicate periods of wetter and colder climates (Alin and Cohen, 2003).

The Grain Size Distribution (GSD) data are primarily generated datasets frequently utilised for sedimentology and other Earth science studies. The end-members are defined as the numerical separation of GSD data into its parts, which provide information on palaeoenvironmental conditions (Weltje and Prins, 2003; Meyer et al., 2013) and also help to understand the sedimentary provenance and depositional regimes/ processes (Paterson and Heslop, 2015). Regarding statistics, the concept of end members is more reliable in describing the depositional habitats. The overall values of end-member modeling analysis (EMMA) have already been extensively documented by Weltje and Prins (2003, 2007). This modeling is an excellent application and functional tool that can eliminate GSDs into geologically relevant sections, estimate end members and be regarded as a nonparametric technique (Paterson and Heslop, 2015).

Study Area and Regional Geology

The Bhimtal region (79°30' to 79°36' E: 29°19' to 29°24' N), covering a part of Survey of India (SOI) Toposheet No. 53 O/11, lies in the Kumaun Lesser Himalaya. The landscape is rough, including large valleys, low and high hills, escarpments, gorges and rivers. The NW-SE extended median part creates a vast step-like valley with numerous lakes and separating terrace-like plains. The steep hills with quartzite caps and trappean rocks beneath them are located east and west of this chain of lakes. These ridges on either side of the diagonal valley represent the two flanks of an asymmetrical anticline.

The Kumaun region of the Lesser Himalaya is home to several lakes, including Bhimtal, Naukuchiatal, and others, which are connected to the active Main Boundary Thrust (MBT) in the south and the Ramgarh Thrust in the north. The Ramgarh Thrust (RT) in the north and the Main Boundary Thrust (MBT) in the south (see Figure 1) are sandwiched by the Lesser Himalayan sequence which exhibits numerous periods of deformation. The Bhimtal area is made up of the rock of the Bhimtal Volcanic formation, which is made

of basalt and is stratigraphically exposed beneath the Bhowali Quartzite (Nagthat Formation), Jantwalgaon and interspersed there in are shale horizons (Valdiya, 1988; Kotlia et al., 1997; Pant and Shukla, 1998) (Figure 1). Presence of a series of depressions linking Bhimtal and Naukuchiatal suggests that these lakes were originally a single large lake (Khanka and Jalal, 1985; Kotlia, 1995). The ancient lake that occupied this low-lying area was likely 7-10 km long and 1 km wide. Further evidence of the lake's existence can be found in the alluvial and lacustrine deposits along the

WNW-ESE trending Nagari-Naukuchiatal valley. Such lakes, formed during the Quaternary period have been described throughout the Himalayas (Kotlia, 1992; Kotlia and Rawat, 2004; Kotlia and Joshi, 2013; Kotlia et al., 1997, 1998, 2000, 2010, 2023; Valdiya et al., 1996; Kothyari et al., 2020).

Field Measurements and Lithostratigraphy

The exposed sequence consists of approximately 9.5 m sediment, including mud, unconsolidated sands, silty clays and gravel (Figure 2). The sequence begins

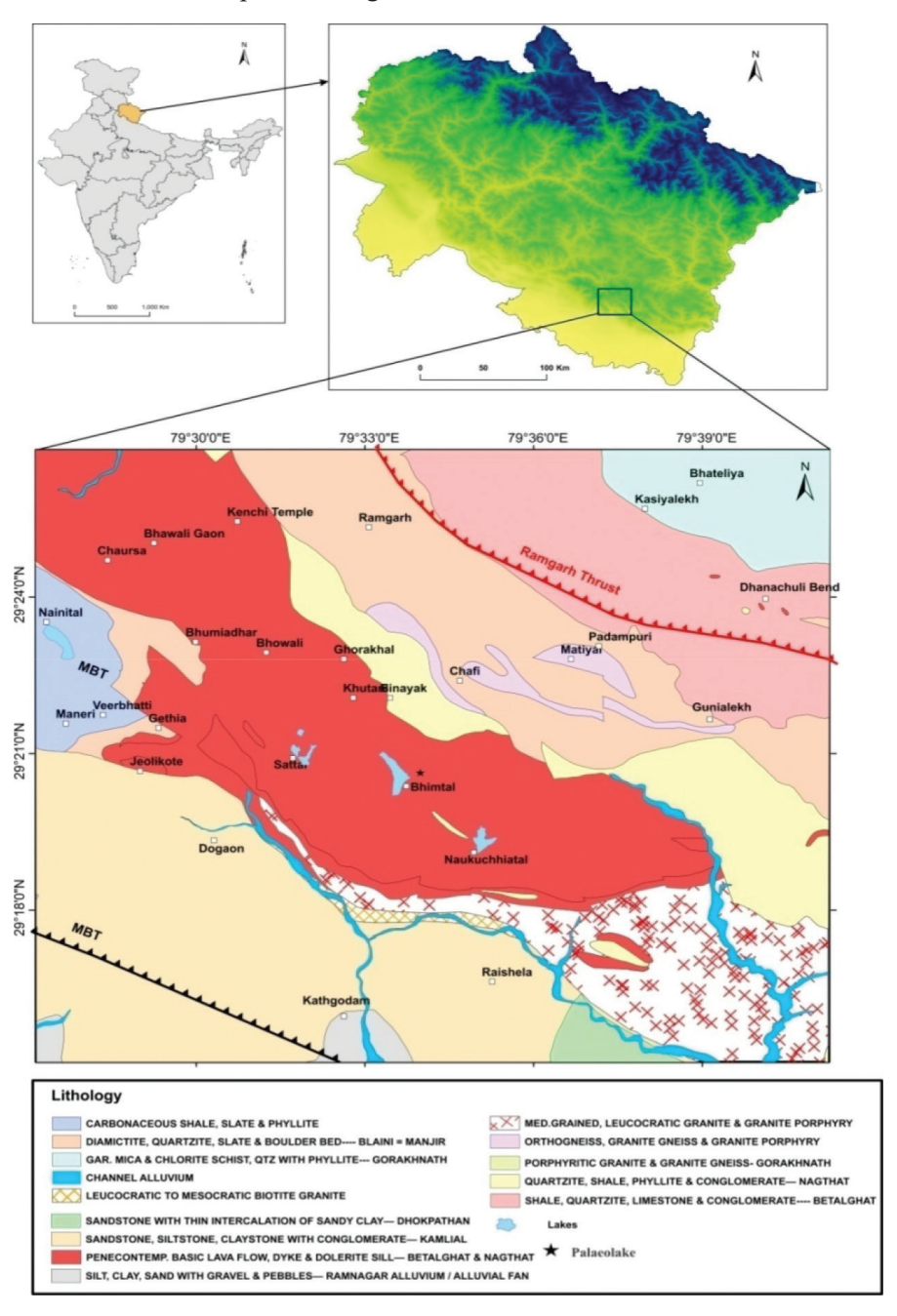


Figure 1: Geological map around the study area.

4

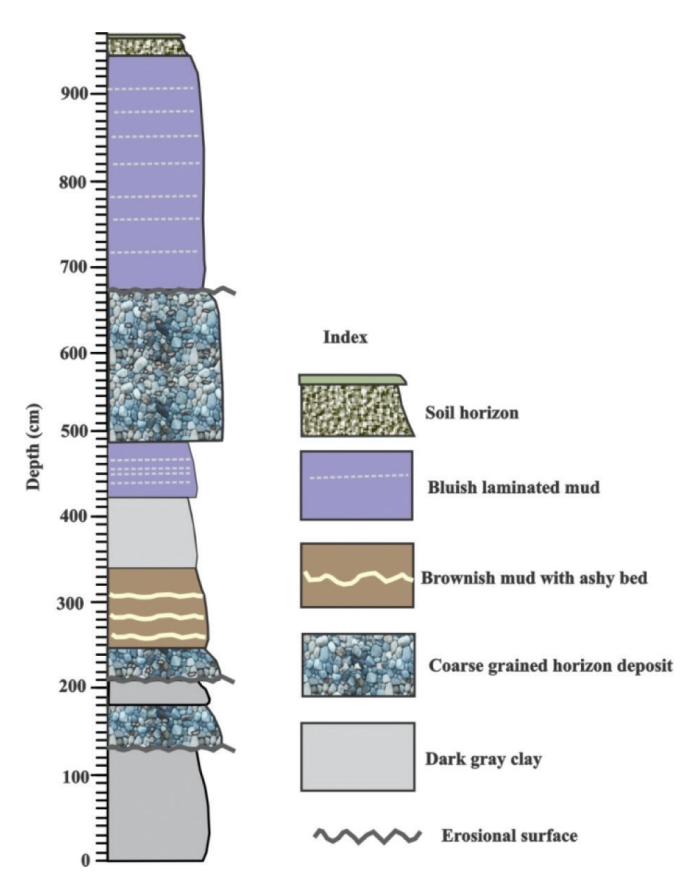


Figure 2: Lithology of Bhimtal palaeolake profile.

with dark grey clay (0-130 cm), representing perhaps moderate energy conditions. Upward from 130 to 180 cm, the section comprises coarse-grained material, followed by dark grey clay from 180 to 210 cm and further followed by a coarse-grained horizon from 210 to 250 cm. From 250 to 340 cm, brownish mud with an scale ashy beds is present, followed by dark grey clay from 340 to 440 cm. From 440 to 480 cm, the profile comprises bluish coloured laminated mud, followed by coarse-grained clay and mud from 480 to 670 cm. The bluish laminated mud is dominant from 670 to 948 cm, and the soil horizon is exposed on the top. A systematic sampling was conducted at 5 cm intervals for comprehensive sedimentological investigations.

Chronology

Four AMS radiocarbon dates were obtained from the Bhimtal palaeolake profile. The AMS radiocarbon dating was performed at NTNU University Museum, Norway. An additional radiocarbon age from Kotlia et al. (1997) was also used for the same profile. The sediment samples were carefully examined under a high-power microscope to remove any micro roots, threads, plastic or other contaminants that could affect the accuracy of the dates. After eliminating the unnecessary material, the samples underwent the Acid-Base-Acid Test (ABA). Subsequently, the samples were freeze-dried for 12 hours, and the dried samples (2 mg) were packed into tin foil capsules. These capsules filled with samples were placed in an auto-sampler for the graphitisation process, and the samples were then subjected to 14C AMS dating using an AMS instrument.

The Age-depth modeling of the obtained radiocarbon ages was performed using OxCal software (version 4.4.4) (Bronk Ramsey, 2009), employing the P_Sequence age-depth model with a variable deposition rate parameter, k (Bronk Ramsey and Lee, 2013). The uncorrected AMS 14C dates were calibrated into years before the present (cal yr BP), specifically 1950 AD. The terrestrial calibration curve IntCal20 was utilized for calibration (Reimer et al., 2020). The calibrated ages ranged from 41,877 cal yr BP (at a depth of 0 cm) to 25,776 cal yr BP (at a depth of 850 cm). The details of the obtained ages are presented in Table 1. The age of the individual zone of the palaeolake was extrapolated with the help of OxCal age depth model. The modeled ages at a 95% confidence interval (2σ) are shown in Figure 3.

Granulometric Analysis

A total of 77 samples were collected for grain size analysis. The standard method for grain size analysis was followed by Kotlia et al. (2023). The samples were dried at 50°C in a hot air oven. Each sample (2 gm) was added to a centrifuge tube containing 10 ml

Table 1: 14C dates obtained on bulk sediments from the Bhimtal palaeolake profile

Lab. no.	Sample depth (cm)	¹⁴ C date (¹⁴ C yr BP)	Calibrated age range (cal yr BP)	Calibrated median age (cal yr BP)
TRa-16468	0	37,337±961	42,944-40,605	41,877
TRa-16471	210	$33,499\pm859$	40,232-36,906	38,587
TRa-16474	445	$31,185\pm286$	36,074-34761	35,470
TRa-16475	485	$27,341\pm205$	31,734-31,107	31,401
RCa	850	$21,500\pm1300$	28,352-23,144	25,776

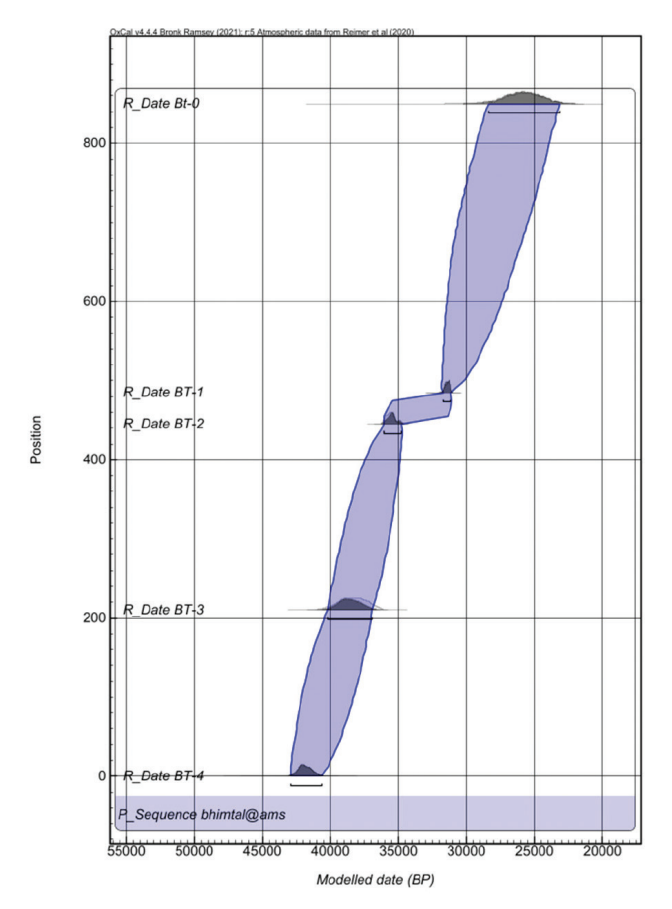


Figure 3: Age depth plot for Bhimtal palaeolake profile using OxCal.

of sodium acetate. The tube was heated for one hour, and this process was repeated twice for each sample. After centrifugation, 2 ml of $\rm H_2O_2$ was added to the sample, followed by boiling for one hour. The sample was then left in a tube overnight. The next day, the samples underwent centrifugation and decanting twice. Subsequently, the samples were treated with sodium bicarbonate (10 ml), sodium citrate (0.2 ml), and sodium dithynide (0.2 gm) and boiled for 1 hour. After three rounds of centrifugation and decanting, the chemically treated samples were ready for further analysis.

The granulometric analysis of the chemically treated samples was performed using a Laser Particle Size Analyzer (LPSA). The data obtained from the analysis was processed using Gradistat software (Blott and Pye, 2001) to conduct further granulometric analysis.

End-Member Modelling Analysis (EMMA)

The MATLAB GUI package AnalySize provides complete capabilities for analysing the GSD data. It processes various data formats obtained from the Particle Size Analyzers instrument (Paterson and Heslop, 2015). The AnalySize can save a fitting

session to a standard MATLAB data file to save time when examining massive data sets. It is an easy user interface for loading the data files and transferring the results to others. In order to distinguish between the various subpopulations within the sediment grain size components, the preferred number of end members was chosen.

Results and Discussion

Grain Size Statistics

Based on the grain size distribution, sediment colour variations and lithofacies, the profile has been divided into nine zones which are labelled as Zone-I to Zone-XI (Figure 4). This division allows for a more comprehensive examination of the sediment characteristics and their variations.

Zone-I (0-30 cm; 41,877-41,460 cal. yr BP). The grain size ranges between 3.7 and 6.1 φ (average 5.4φ), indicating a composition of medium silt to very fine sand. The silt, sand and clay components are present at 70.2%, 22.5% and 7.6%, respectively. The sand percentage ranges from 9.9% to 56.2%, the silt from 39.5% to 81.7%, and the clay from 4.3% to 9.3% (Figure 4). The high sandy silt concentration indicates a high-energy depositional environment and suggests low rainfall situation in the catchment (e.g., Warrier et al., 2013). The sediment types in Zone-I vary from unimodal to bimodal, and its texture is classified as sandy mud.

Zone-II (30-110 cm; 41,460- 40,170 cal. yr BP). The grain size varies from 4.7 to 6.6φ (average 5.7φ), indicating medium silt to coarse silt. The sediment comprises an average value of sand at 18.0%, silt at 73.7% and clay at 8.3% with silt being the significant component. The content of sand varies between 5.6-39.5%, while the silt and clay concentrations range between 55.8-83.1% and 4.7-12.9%, respectively (Figure 4). The highest sandy silt concentration indicates high-energy environmental conditions during the sediment deposition. It also reveals lower rainfall in Zone II as compared to Zone I. The sample types vary between unimodal and bimodal in nature, and their texture is classified as mud to sandy mud.

Zone-III (110-190 cm; 40,170-38,890 cal. yr BP). The size of the grain varies from 4.3 to 6.9φ (average 5.6φ). The dominant components are silt (66.0%), followed by sand (18.0%) and clay (7.4%). The sand percentage varies between 3.9 and 55.3%, the silt ranges from 41.1 to 84.7% and the clay ranges from 3.6 to 11.4% (Figure 4). The silt concentration in this

zone is the highest, suggesting high precipitation and low-energy environmental condition. The sample type in Zone-III is unimodal and bimodal, with a texture of sandy mud to muddy sand in nature.

Zone-IV (190-290 cm; 38,890-37,460 cal. yr BP). The grain size distribution ranges from 4.4 to 6.4φ (average 5.6φ), showing a concentration of silt from medium to very coarse in size. The sediment comprises sand at 22.1%, silt at 74.9%, and clay at 6.7%, with silt being the primary constituent, followed by sandy clay. The percentage of sand varies between 3.8 and 41.9%, while silt and clay are present in relatively minor amounts, ranging from 55.6 to 85.7% and 2.5 to 10.5%, respectively (Figure 4). The high sandy silt concentration suggests a high-energy environmental condition and indicates less precipitation or dry conditions in the catchment. The sample type is unimodal and bimodal in this zone, with a sandy mud-to-mud texture.

Zone-V (290-440 cm; 37,460-35,510 cal. yr BP). The mean size of grain ranges between 4.6 and 6.5 φ (average 5.4φ), indicating medium silt and very coarse silt. The sediment consists of an average of 26.3% sand, 66.8% silt and 6.8% clay, with silt being the significant constituent, followed by sand and clay. Sand percentages vary between 5.0 and 43.6%, while silt (51.3-85.3%) and clay (3.8-10.3%) also vary (Figure 4). The high sandy silt concentration suggests that the sediment was deposited under the high-energy depositional conditions, which may be coupled with low precipitation or dry climatic conditions. The sample types in Zone-V are unimodal, bimodal and polymodal, with a texture of sandy mud to mud.

Zone-VI (440-590 cm; 35,510-29,970 cal. yr BP). It is characterised by an average grain size ranging from 3.4 to 6.8φ (average 5.3φ), indicating medium silt to very fine sand. The composition is characterised by silt as a significant constituent, followed by sand and clay, with average sand (28.0%), silt (65.2%) and clay (6.8%). The sand concentration varies widely from 4.3 to 70.2%, while the silt (26.9-70.5%) and clay (2.9-13.5%) contents are relatively consistent (Figure 4). The high sandy silt concentration suggests a depositional environment with high energy and low rainfall or dry climatic conditions. Zone-VI ranges from unimodal to bimodal and belongs to the texture of sandy mud to mud in nature.

Zone-VII (590-710 cm; 29,970-28,000 cal. yr BP). The size of the grain varies between 4.3 and 7.8φ (average 6.6φ) with a composition of very coarse silt to fine silt. The mean values of silt, sand, and clay contents are 75.8%, 12.9%, and 11.3%, respectively, with silt

as the primary constituent, followed by sand and clay content. The concentration of sand has a range from 0.0 to 60.9%, while silt (36.6-89.5%) and clay (2.5-19.9%) are also present (Figure 4). The high silt concentration suggests that the sediment was deposited under low energy conditions and moist climatic conditions. The sample types in Zone-VII are unimodal, bimodal and trimodal, with a texture of sandy mud to mud.

Zone-VIII (710-870 cm; 28,000-25,450 cal. yr BP). This zone is characterised by grains ranging from 6.3 to 7.6φ (average 7.1φ) with medium to fine silt. The composition consists of 2.3% sand, 85.9% silt, and 11.8% clay, with silt as the primary component, followed by sand and clay. The sand concentration fluctuates between 0.0 and 9.6%, while silt (81.0-92.0%) and clay (7.4-16.5%) also fluctuate (Figure 4). The highest silt concentration reflects a low-energy environmental condition related to high precipitation or wetter climatic situations. The sample types in Zone-VIII are unimodal, bimodal, and trimodal with a texture of mud.

Zone-IX (870-948 cm; 25,450-24,230 cal. yr BP). It has a mean grain size between 3.5 and 7.6φ (average 6.6φ) and is composed of fine silt to very fine sand. Silt is the significant component, with an average concentration of 79.2%, followed by sand at 10.6% and clay at 10.2%. The sand concentration fluctuates between 0.0 and 61.7%, while the silt and clay concentrations range from 34.5 to 89.4% and 3.9 to 15.3%, respectively (Figure 4). The high concentration of silt suggests a low-energy depositional environment characterized by high rainfall and wet climatic conditions during deposition. The sediment samples exhibit unimodal to bimodal distribution. The textural group of the sediment ranges from mud to muddy sand, indicating a mixture of fine particles (mud) and coarser particles (muddy sand).

Our data on the concentration of grain size indicate that the deposition of the Bhimtal Lake sediments predominantly occurred in a high-energy environmental regime. Zones I, II, IV, V and VI specifically experienced high-energy conditions, under an arid environment. As a result, the lake area would have contracted, and the shoreline would have moved closer to the lake's center. This proximity to the shoreline led to the deposition of coarser sediments (e.g., Finney and Johnson, 1991; Shuman et al., 2001). On the other hand, zones III, VII, VIII and IX exhibit low-energy conditions, indicating high lake level during sediment deposition due to increased precipitation. In this climate, the lake level would have risen and expanded, allowing

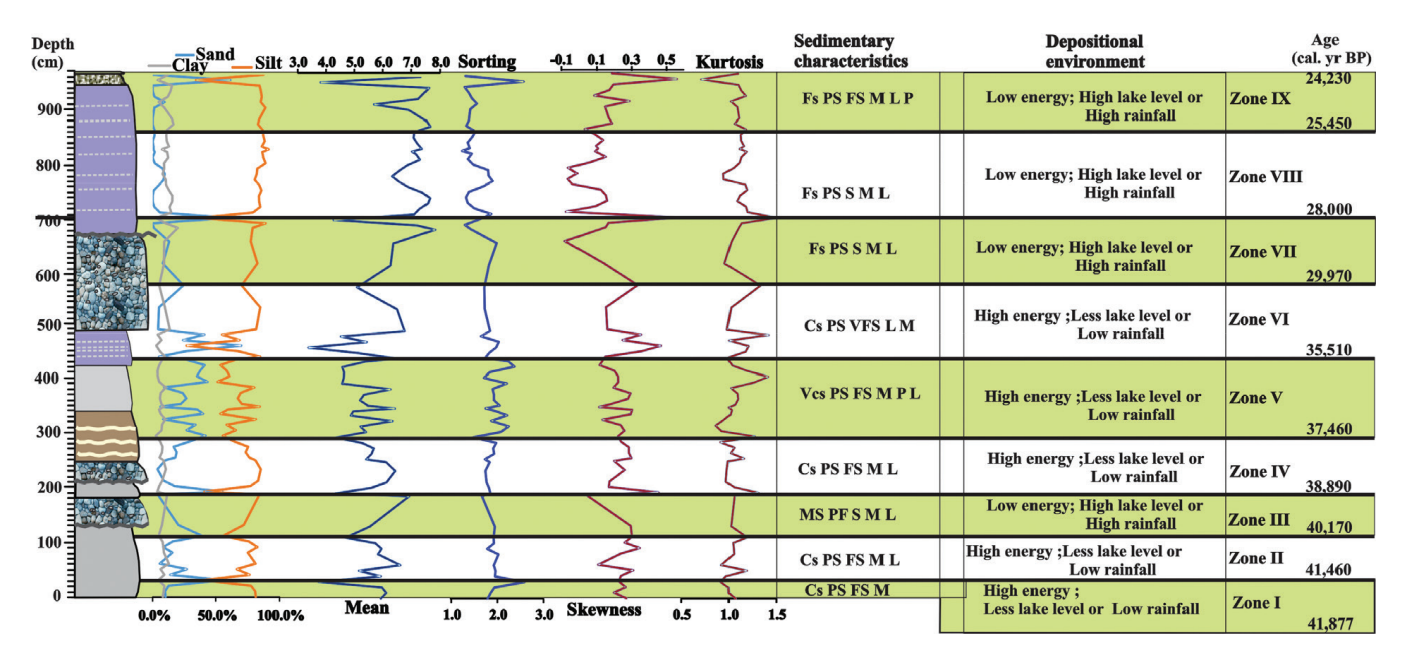


Figure 4: Bhimtal palaeolake sediments exhibiting variations in composition of sand, silt, and clay, expressed as percentages. The sediments display mean grain size, sorting, skewness, kurtosis, sedimentary characteristics and the environment of deposition. Vcs= very coarse silt, Ms= medium silt, Cs= coarse silt, PS= poorly sorted, FS= fine skewed, S= symmetrical, M= mesokurtic, L= leptokurtic, P= platykurtic.

for the deposition of fine particles. The coarser particles, however, would have been deposited closer to the lake shore (e.g., Menking, 1997; Chen and Wan, 1999).

Bivariate Plots

Bivariate plots are used to examine the relationship between two variables and can be used to understand the relationship between grain size and other sediment characteristics, such as energy conditions, depositional settings, hydrodynamic conditions and deposition agents. These plots can provide essential insights into the processes that led to sediment formation and help interpret depositional environments.

Relationship Between Mean size (Mz) Versus Sorting

The mean vs. standard deviation plot (Figure 5a) illustrates that the sediments are distributed across a region, indicating poor sorting. This distribution suggests that a majority of the samples exhibit low levels of sorting. As the mean grain size transitions from sand to silt, the level of sorting decreases. Poorly sorted sediments indicate that they were deposited in a low-energy environment (Blot and Pye, 2001; Padhi et al., 2017; Kotlia et al., 2023).

Relationship Between Mean size (Mz) and Kurtosis (KG)

Based on the bivariate plot of mean size and kurtosis (Figure 5b), most sediments exhibit a mesokurtic nature with kurtosis values ranging from 0.9 to 1.1. The mean size varies from very fine sand to medium silt, exhibiting a highly mesokurtic distribution. In contrast, the remaining section, consisting primarily of silt, exhibits distributions ranging from leptokurtic to platykurtic. The sand units specifically demonstrate a platykurtic distribution.

Relationship Between Mean size (Mz) and Skewness (SK)

Based on the bivariate plot of mean size and skewness (Figure 5c), it can be observed that the skewness values exhibit a range from very fine to symmetrical. The very fine skewed values ranged from 0.2 to 1.2, the fine skewed values from 0.3 to 0.1, very fine skewed values from 0.3 to 0.6, and symmetrical skewed values fell between -0.1 and 0.1. The grouping of sediments within the fine-skewed zone, as depicted in Figure 5c, suggests the presence of finely skewed sediments. This skewness is a result of the inclusion of silt particles into the sand component.

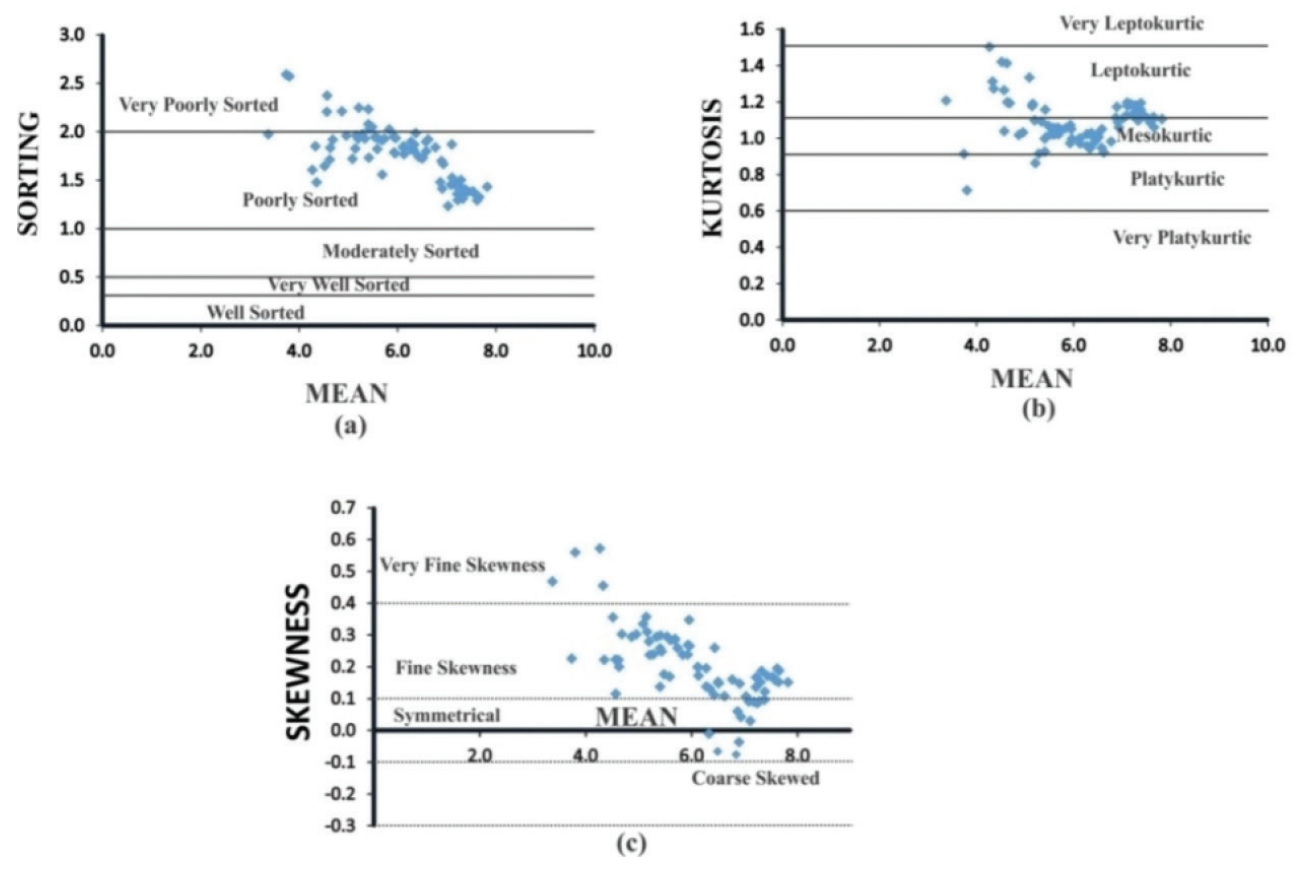


Figure 5: Bivariate plots: (a) mean vs. sorting, (b) mean vs. kurtosis, (c) mean vs. skewness.

End Member Modelling Analysis (EMMA)

The EMMA of the Bhimtal sediment profile was carried out to understand the end-members (EM) that help to understand the sedimentation process by analyzing different grain-size parameters, distribution and the different modes of end-members. The grain size data depicts ranges in clay from ~2.5 to 20% (average=8.90%), silt ~27–92% (average = 74.50%) and fine sand fractions of $\sim 0-70\%$ (average= 16.60%) (Figure 6). The EM1 exhibits a dominant mode peak at around 2 \$\phi\$ (very fine silt and clay). It varies from 0 to 100% (average = 47%). The EM2 exhibits a symmetrical unimodal peak in the very coarse silt range (mode at 3.5ϕ) with proportions ranging from 0-77% (average = 35%). The EM3 is characterized by an asymmetrical unimodal peak centered around 4.4 \phi (fine sand) from 0-92% (average = 13%), and EM4 exhibits a bimodal structure with a dominant mode at around 5.3 ϕ (coarse sand) from 0–87% with an average of 6%. The EM4 also shows additional minor modes. The EM1 has an average fractional abundance of 4.6, which is dominant in bluish-colour laminated mud rich in clay and fine silt for the lithologic unit. The EM2

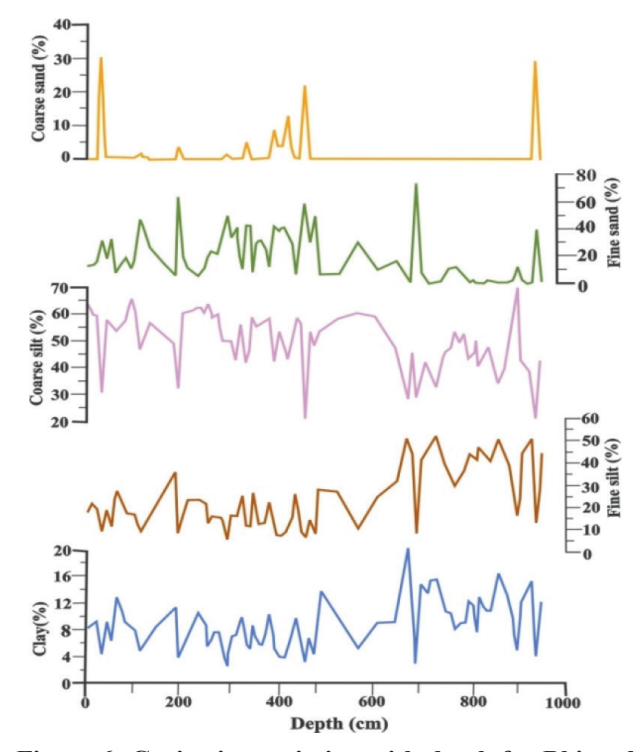


Figure 6: Grain size variation with depth for Bhimtal lake profile.

exhibits high coarse silt and clay representing brownish mud with an ashy bed and relatively high in dark grey silty clay and landslide materials (average 5.4). The third end-member (EM3) displays relatively low values in bluish laminated mud and comparatively high values in dark grey clay and brownish mud (average of 6.3). EM4 is only recorded in a few layers of dark grey clay with an average value of 5.10 (Figure 7).

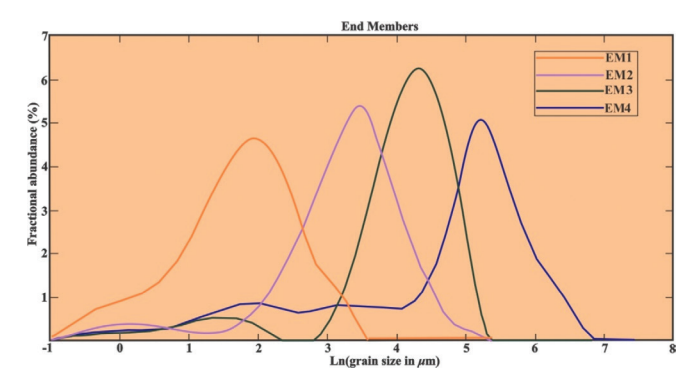


Figure 7: Energy model diagram of Bhimtal profile showing variation with different energy conditions (EM1 – EM4) with depth.

The end members (EM) help to identify transportation processes and sediment flux to the lake for model analysis. Four end members (EM1, EM2, EM3 and EM4) extracted from energy modelling reflect the lake's energy conditions as shown in Figure 8. The EM1 shows the clay to fine silt-sized fraction, which deliberates less water supply into the lake and corresponds to higher lake levels under warm-wet climatic conditions. The EM2 is indicated by the more significant deposition of coarse silt fraction components, reflecting a very shallow lake environment in moderate energy conditions. The EM3 and EM4 represent fine to coarse sand fractions during shallow lake-level conditions, possibly under drier climatic conditions with higher energy flow. The EM3 is opposite to EM2 from 0 to 500 cm and shows similar trends with EM1 from 500 to 700 cm depth (Figure 8). The energy model of the lake provides the changes in the hydrological energy conditions of the catchment area and the transportation medium. These conditions help to interpret the data with past climate and palaeoenvironmental conditions. During the warm and wet climate, the lake water level is higher. The sediment inflow intensity into the lake's center is significantly reduced and only provides low energy transported suspended load of finer fractions deposited as fine silt and clay. Under colder and drier climatic conditions with high energy flow and low lake

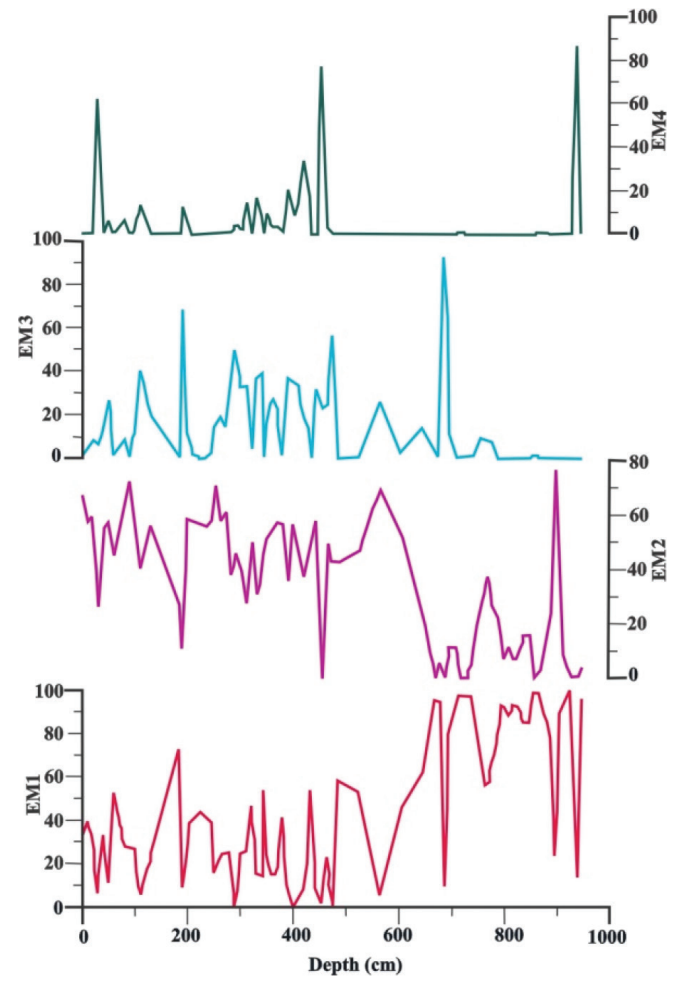


Figure 8: Results of end-member modelling (EM1-EM4) using grain size data of Bhimtal lake profile. End-member represent unmixed grain-size distributions of four end members EM1, EM2, EM3, and EM4. EM1; low energy conditions, EM2; very shallow lake environment in moderate energy conditions, and EM3 and EM4; fine to coarse sand fractions during shallow lake-level conditions showing high energy conditions.

level, the higher grain size fractions are transported quickly and deposited in the lake.

Conclusion

The grain-size studies demonstrate that the predominance of sediments is unimodal. The unimodal distribution of palaeolake sediments demonstrates that they were supplied by fluvial action. From the ternary plot diagram, we can infer that silt predominates, followed by sand and clay. Accumulation of fine silt indicates a warm climate and high lake level because of substantial monsoon. In contrast, coarse sand-sized particles indicate relatively cold phase and shallow

lake-level conditions. Except for Zones III, VII, VIII and IX, the zone-wise distribution of the entire profile indicates that sandy silt concentration is highest in other zones. Higher concentrations of sandy silt represent high-energy depositional conditions during sediment deposition. It also implies that the catchments have low rainfall or a dry climate with low lake levels. Higher concentrations of silt in Zones III, VII, VIII, and IX indicate low-energy depositional environments, high lake levels and high rainfall in moist climates. The standard deviation results indicate that the sediment is poorly sorted, concluding that sediment is transported from the proximal source and deposited under lowenergy environmental conditions. The kurtosis value indicates that the samples are leptokurtic, platykurtic and mesokurtic in nature which indicates changes in the flow characteristics of the depositional medium. The skewness value of the sediment sample indicates that samples are symmetrical to very finely skewed, and the variability in the skewness values suggests changes in the hydrodynamic conditions of the lake. The bivariate plot also suggests that the sediment is mostly finely skewed and poorly sorted with leptokurtic. The end member analysis suggests that EM1 and EM2 are opposite except from depths 400 to 500 cm. The EM3 shows the opposite to EM2 from 0 to 500 cm and similar trends with EM1 from depths 500 to 700 cm. The approach of EMMA provides a means of unraveling sediment fluxes from catchment areas and other sources, opening the way to significant advances in palaeoclimatic reconstructions from sediment grainsize distribution data. In general, Bhimtal palaeolake sediments are generally rich in silt-sized fractions.

Author's Contribution

The research was conceived by BSK. Field work was carried out by BSK, AKS and LMJ. The sample analysis was performed by MK, AKS, AS, BP and RK. The manuscript was written by BSK, MK and BP with input from HB, AS, PC, KG and AM.

References

- Adrian, R., O'Reilly, C.M., Zagarese, H., Baines, S.B., Hessen, D.O., Keller, W., Livingstone, D.M., Sommaruga, R., Straile, D., van Donk, E., Weyhenmeyer, G.A., and Winder, M., 2009. Lakes as sentinels of climate change. *Limnology and Oceanography*, 54: 2283-2297.
- Alin, S.R. and Cohen, A.S., 2003. Lake-level history of Lake Tanganyika, East Africa, for the past 2500

- years based on ostracode-inferred water-depth reconstruction. *Palaeogeography Palaeoclimatology Palaeoecology*, **199:** 31-49.
- Bird, B.W., Polisar, P.J., Lei, Y., Thompson, L.G., Yao, T., Finney, B.P., Bain, D.J., Pompeani, D.P. and Steinman, B.A., 2014. A Tibetan lake sediment record of Holocene Indian summer monsoon variability. *Earth and Planetary Science Letters*, **399**: 92-102.
- Blott, S.J and Pye, K., 2001. Gradistat: a grain size distribution and statistics package for the analysis of unconsolidated sediments. *Earth Surface Processes Landforms*, **26:** 1237-1248.
- Bronk Ramsey, C. 2008. Deposition models for chronological records. *Quaternary Science Reviews*, **27:** 42-60.
- Bronk Ramsey, C., 2009. Bayesian analysis of radiocarbon dates. *Radiocarbon*, **51:** 37-60.
- Bronk Ramsey, C. and Lee, S., 2013. Recent and planned developments of the program OxCal. *Radiocarbon*, **55**: 720-730.
- Chen, J. and Wan, G., 1999. Sediment particle size distribution and its environmental significance in Lake Erhai, Yunnan Province. *Chinese Journal of Geochemistry*, **18:** 314-320.
- Chen, J.A., Wan, G., Zhang, D.D., Zhang, F. and Huang, R., 2004. Environmental records of lacustrine sediments in different time scales: Sediment grain size as an example. Science in China Series D: Earth Sciences, 47: 954-960.
- Flemming, B.W. 2007. The influence of grain-size analysis methods and sediment mixing on curve shapes and textural parameters: Implications for sediment trend analysis. *Sedimentary Geology*, **202**, 425-435.
- Folk, R.L. and Ward, W.C., 1957. Brazos River Bar: A study in the significance of grain size parameters. *Journal of Sedimentary Petrology*, **27:** 3-26.
- Finney, B.P. and Johnson, T.C., 1991. Sedimentation in Lake Malawi (East Africa) during the past 10,000 years: A continuous paleoclimatic record from the southern tropic. *Palaeogeography Palaeoclimatology Palaeoecology*, **85**: 351-366.
- Khanka, L.S. and Jalal, D.S., 1985. Bathymetric analysis of lake Bhimtal, Kumaun Himalaya. *In:* J.S. Singh (Editors), Environmental Regeneration in Himalaya: Concepts and Strategies. pp.435-439.
- Kothyari, G.C., Kotlia, B.S., Talukdar, R., Pant, C.C., Joshi, M., 2020. Evidences of neotectonic activity along Goriganga River, higher central Kumaun Himalaya, India. *Geological Journal*, **55(9)**: 6123-6146, https://doi.org/10.1002/gj.3791.
- Kotlia, B.S., 1995. Upper Pleistocene Soricidae and Muridae from Bhimtal-Bilaspur deposits, Kumaun Himalaya, India. *Journal of Geological Society of India*, **40(6)**: 155-171.
- Kotlia, B.S., 1992. Pliocene murids (Rodentia, Mammalia) from Kashmir basin, northwestern India. *Neues Jahrbuch für Geol.Paläontol. Abhandlungen*, **184:** 339-357.
- Kotlia, B.S. and Joshi, L.M., 2013. Neotectonic and climatic impressions in the zone of Trans Himadri Fault (THF),

- Kumaun Tethys Himalaya, India: A case study from palaeolake deposits. *Zeitschrift für Geomorphologie*, **57**: 289-303.
- Kotlia, B.S., Kukreti, M., Bisht, H., Singh, A.K., Sharma, A., Kothyari,G. C., Porinchu, D.F., Chand, P., Kashyap, R. and Sharma, G.K., 2023. Palaeoenvironmental reconstruction through granulometric analysis of a palaeolake deposit at Bhikiyasain, Kumaun Lesser Himalaya. *Journal of Climate Change*, 9(1): 25-37.
- Kotlia, B.S. and Rawat, K.S., 2004. Soft sediment deformation structures in the Garbyang palaeolake: Evidence for the past shaking events in the Kumaun Tethys Himalaya. *Current Science*, **87**: 377-379.
- Kotlia, B.S., Sanwal, J., Phartiyal, B., Joshi, L.M., Trivedi, A. and Sharma, C., 2010. Late Quaternary climatic changes in the eastern Kumaun Himalaya, India, as deduced from multi-proxy studies. *Quaternary International*, 213 (1-2): 44-55.
- Kotlia, B.S., Schallreuter, I.H., Schallreuter, R. and Schwarz, J., 1998. Evolution of Lamayuru palaeolake in the Trans Himalaya: Palaeoecological implications. *E&G Quaternary Science Journal*, **48(1)**: 177-191.
- Kotlia, B.S., Sharma, C., Bhalla, M.S., Rajagopalan, G., Subrahmanyam, K., Bhattacharyya, A. and Valdiya, K.S., 2000. Palaeoclimatic conditions in the Late Pleistocene Wadda Lake, eastern Kumaun Himalaya, India. Palaeogeography Palaeoclimatology Palaeoecology, 162: 105-118.
- Kotlia, B.S., Shukla, U.K., Bhalla, M.S., Mathur, P.D. and Pant, C.C., 1997. Quaternary vfluvio-lacustrine deposits of the Lamayuru basin, Ladakh Himalaya: Preliminary multidisciplinary investigations. *Geological Magazine*, **134(6):** 807-815.
- Menking, K.M., 1997. Climatic signals in clay mineralogy and grain-size variations in Owens Lake core OL-92, southeast California. *In*: Smith, G.I., Bischoff, J.L.(Eds.), An 800,000 Year paleoclimatic record from core OL-92, Owens Lake, Southeast California, *Geological Society of America, Special Paper*, **317**: 37-48.
- Meyer, I., Davies, G.R., Vogt, C., Kuhlmann, H. and Stuut, J.B.W., 2013. Changing rainfall patterns in NW Africa since the Younger Dryas. *Aeolian Research*, **10**: 111-123.
- Padhi, D., Singarasubramanaian, S.R., Panda, S. and Venkatesan, S., 2017. Depositional mechanism as revealed from Grain size measures of Rameswaram coast, Ramanathpuram District, Tamil Nadu, India. *International Journal of Theoretical Applied Sciences*, **9(2)**: 168-177.
- Paterson, G.A. and Heslop, D., 2015. New methods for unmixing sediment grain size data. *Geochemist Geophysics, Geosystems*, **16:** 4494-4506.
- Rawat, V., Rawat, S., Srivastava, P., Negi, P.S., Prakasam, M. and Kotlia, B.S., 2021. Middle Holocene Indian summer monsoon variability and its impact on cultural changes in the Indian subcontinent. *Quaternary Science Reviews*, 255: 106825.

- Reimer, P.J., Austin, W.E.N., Bard, E., Bayliss, A., Blackwell, P., Bronk Ramsey, C., Butzin, M., Cheng, H., Edwards, R.L., Friedrich, M., Grootes, P.M., Guilderson, T.P., Hajdas, I., Heaton, T.J., Hogg, A.G., Hughen, K.A., Kromer, B., Manning, S.W., Muscheler, R., Palmer, J.G., Pearson, C., van der Plicht, J., Reimer, R.W., Richards, D.A., Scott, E.M., Southon, J.R., Turney, C.S. M., Wacker, L., Adolphi, F., Büntgen, U., Capano, M., Fahrni, S., Fogtmann-Schultz, A., Friedrich, R., Kudsk, S., Miyake, F., Olsen, J., Reinig, F., Sakamoto, M., Sookdeo, A. and Talamo, S., 2020. The IntCal20 Northern Hemispheric radiocarbon calibration curve (0–55 kcal BP). *Radiocarbon*, 62: 725-757.
- Sinha, A.K. and Pal, D., 1978. Ecological problems in the high altitude lakes of Nainital area: Problems and suggestions. *Journal of Himalayan Studies*, **2:** 39-43.
- Shuman, B., Bravo, J., Kaye, J., Lynch, J.A., Newby, P. and Webb, T., 2001. Late Quaternary water-level variations and vegetation history at Crooked Pond, southeastern Massachusetts. *Quaternary Research*, **56:** 401-410.
- Valdiya, K.S., 1988. Geology and Natural Environment of Nainital Hills, Kumaun Himalaya, Nainital, Gyanodaya Prakashan, pp. 158.
- Valdiya, K.S., Kotlia, B.S., Pant, P.D., Shah, M., Mungali, N., Tewari, S. and Upreti, M., 1996. Quaternary palaeolakes in Kumaun Lesser Himalaya: finds of neotectonic and palaeoclimatic significance. *Current Science* 70 (2): 157-161.
- Verkulich, S.R. and Melles, M., 1992. Composition and paleoenvironmental implications of sediments in a fresh water lake and in marine basins of Bunger Hills, East Antarctica. *Polarforschung*, **60**: 169-180.
- Vriend, M., Prins, M.A., Buylaert, J.P., Vandenberghe, J. and Lu, H., 2011. Contrasting dust supply patterns across the north-western Chinese Loess Plateau during the last glacial-interglacial cycle. *Quaternary International*, 240: 167-180.
- Wang, N., Ning, K., Li, Z., Wang, Y., Jia, P. and Ma, L., 2016. Holocene High Lake-levels and Pan-lake Period on BadainJaran Desert. *Science China Earth Sciences*, **59:** 1633-1641.
- Wang, H., Li, H., Si, J., Zhang, L. and Sun, Z., 2019. Geochemical features of the pseudotachylytes in the Longmen Shan thrust belt, eastern Tibet. *Quaternary International*, **514**: 173-185.
- Warrier A.K, Shankar R. and Sandeep K., 2013. Sedimentological and carbonate data evidence for lake level variations during the past 3700 years from a southern Indian lake. *Palaeogeography, Palaeoclimatology, Palaeoecology*, **397:** 52-60.
- Weltje, G.J. and Prins, M.A., 2003. Muddled or mixed? Inferring palaeoclimate from size distributions of deep-sea clastics. *Sedimentary Geology*, **162**: 39-62.
- Weltje, G.J. and Prins, M.A., 2007. Genetically meaningful decomposition of grain-size distributions. *Sedimentary Geology*, **202(3)**: 409-424.